Journal of Hazardous Materials 180 (2010) 217–224

Contents lists available at ScienceDirect

Journal of Hazardous Materials

journal homepage: www.elsevier.com/locate/jhazmat

Adsorption treatment of oxide chemical mechanical polishing wastewater from a semiconductor manufacturing plant by electrocoagulation

Wei-Lung Chou[a,*], Chih-Ta Wang[b], Wen-Chun Chang[a], Shih-Yu Chang[a]

[a] Department of Safety, Health and Environmental Engineering, Hungkuang University, No. 34, Chung-Chie Road, Sha-Lu, Taichung 433, Taiwan
[b] Department of Safety Health and Environmental Engineering, Chung Hwa University of Medical Technology, Tainan Hsien 717, Taiwan

ARTICLE INFO

Article history:
Received 25 October 2009
Received in revised form 2 March 2010
Accepted 7 April 2010
Available online 13 April 2010

Keywords:
Electrocoagulation
Wastewater treatment
Chemical mechanical polishing (CMP)
Adsorption kinetics
Adsorption isotherms
Thermodynamics

ABSTRACT

In this study, metal hydroxides generated during electrocoagulation (EC) were used to remove the chemical oxygen demand (COD) of oxide chemical mechanical polishing (oxide-CMP) wastewater from a semiconductor manufacturing plant by EC. Adsorption studies were conducted in a batch system for various current densities and temperatures. The COD concentration in the oxide-CMP wastewater was effectively removed and decreased by more than 90%, resulting in a final wastewater COD concentration that was below the Taiwan discharge standard (100 mg L^{-1}). Since the processed wastewater quality exceeded the direct discharge standard, the effluent could be considered for reuse. The adsorption kinetic studies showed that the EC process was best described using the pseudo-second-order kinetic model at the various current densities and temperatures. The experimental data were also tested against different adsorption isotherm models to describe the EC process. The Freundlich adsorption isotherm model predictions matched satisfactorily with the experimental observations. Thermodynamic parameters, including the Gibbs free energy, enthalpy, and entropy, indicated that the COD adsorption of oxide-CMP wastewater on metal hydroxides was feasible, spontaneous and endothermic in the temperature range of 288–318 K.

1. Introduction

The semiconductor industry has become a representative industry in Taiwan. Chemical mechanical polishing (CMP) is a major semiconductor manufacturing process, entailing micro-polishing used to obtain uniform surfaces of inter-metal dielectrics (IMD) or inter-level dielectrics (ILD) during integrated circuit (IC) fabrication [1]. CMP ensures both the local and global flatness of a semiconductor surface via the mechanical downward force of a slurry abrasive and the chemical oxidation of the wafer surface. Because of the abrasive slurry used in the CMP process, a large amount of water is required to wash out the abrasives that have adhered to the wafer surface. As a result, correspondingly large quantities of wastewater and sludge are produced and released into the environment [2].

CMP wastewater is highly alkaline and turbid with high total solids content. In addition, untreated CMP wastewater is rich in organic matter, which leads to an increased concentration of these microorganisms. The inorganic and organic contaminants in the CMP effluent derive primarily from the CMP slurry [3]. Inorganic contaminants may contain suspended, nano-sized solids generated from abrasive slurry particles of SiO_2, Al_2O_3, or CeO_2, depending on the nature of the CMP application. Organic contaminants may include metal oxidizing agents, additives, dispersing agents, and rheology control agents [4]. Chemical oxygen demand (COD) is a measure of the amount of oxygen used in chemical oxidation of inorganic and organic matter contained in wastewater. Although COD is not the only parameter to measure pollution, it is considered an indicator of the degree of pollution in the effluent and of the potential environmental impact of wastewater discharge. CMP wastewater contains suspended particles with highly negative surface charges that repel adjacent particles when they are immersed in alkaline solutions. Because of these characteristics of CMP wastewater, removing such nano-sized particles by conventional chemical coagulation is not ideal. Therefore, there is an urgent need to develop more efficient techniques for the treatment of CMP wastewater.

Electrochemical method has attracted considerable attention because of its environmental compatibility. Electrons are considered a “clean reagent” [5]. Thus, an electrocoagulation (EC) technology has been proposed to treat wastewater containing dispersed fine particles without the need for additional chemicals [6]. This technique has some advantages as compared to conventional methods: easier operation, simpler equipment, lower retention time, lower sludge production, and better safety [7]. EC is a process

* Corresponding author. Tel.: +886 4 26318652x4005; fax: +886 4 26319175.
E-mail address: wlchou@sunrise.hk.edu.tw (W.-L. Chou).

0304-3894/$ – see front matter © 2010 Elsevier B.V. All rights reserved.
doi:10.1016/j.jhazmat.2010.04.017

that generates metallic hydroxides *in situ* via electro-dissolution of a soluble sacrificial anode immersed in the wastewater. The electrochemically generated metallic ions hydrolyze near the anode to form a series of metal hydroxides that are able to destabilize dispersed particles present in the wastewater to be treated. The destabilized particles are believed to be responsible for the aggregation and precipitation of suspended particles and the adsorption of dissolved pollutants. EC has emerged as a technique in treating potable water [8], urban wastewater [9], metal laden wastewater [10], dyeing wastewater [11], restaurant wastewater [12], chemical mechanical polishing wastewater [6,13–15], and wastewater containing phosphates [16], fluoride [17], arsenic [18], indium [19,20], and polyvinyl alcohol [21–23]. Previous research has primarily studied removal characteristics and CMP wastewater quality before and after electrocoagulation treatment [6,13–15]. To our knowledge so far, little information is available on the adsorption of COD in oxide-CMP wastewater onto metal hydroxides produced during the EC process.

Metal hydroxides generated during EC were used to remove the COD of oxide-CMP wastewater from a semiconductor manufacturing plant in central Taiwan by electrocoagulation. The adsorption kinetics of the electrocoagulants was analyzed using pseudo-first- and second-order kinetic models at various current densities and temperatures. The equilibrium adsorption behavior was analyzed and compared to the model predictions of the Langmuir, Freundlich and Dubinin–Raduskevich (D–R) isotherms. The effect of temperature on the adsorption isotherms was determined, and the thermodynamic parameters during the adsorption such as the free energy, enthalpy and entropy were calculated for the various temperatures.

2. Experimental

2.1. Materials and apparatus

Oxide-CMP wastewater was obtained from a dynamic random access memory (DRAM) manufacturing unit in the Central Taiwan Science Park, Taichung, Taiwan. The concentration of the supporting electrolyte in the aqueous solutions was adjusted by adding NaCl (Tedia Company, USA). Fig. 1 shows a schematic diagram of the experimental apparatus and electrode assembly for the EC system. The electrolytic cell was a 1.0 L Pyrex® glass vessel equipped with a water jacket and magnetic stirrer (Suntex, SH-301, Taiwan). The temperature of the electrolytic cell was controlled by continuously circulating water from a refrigerated circulating bath (Model BL-720, Taiwan) through the water jacket. From our previous studies on oxide-CMP wastewater, a cast iron (Fe)/aluminum (Al) electrode pair (8 cm × 6 cm × 0.3 cm) is known to be the optimum choice of electrode pair combination (Fe/Al, Fe/Fe, Al/Al, and Al/Fe) as the anode/cathode pair [13–15]. The electrode pair was immersed in wastewater to a depth of 5.2 cm with the electrodes around 2 cm apart. The effective area of the electrode pair was 31.2 cm^2. The assembly was connected to a direct current power source (2400 Series Sourcemeter, Cleveland, OH, USA) with a galvanostatic mode. Characteristics of the oxide-CMP wastewater, such as pH (Y.S.I, pH 10, USA), conductivity (Eutech, Cyberscan 510, Singapore), turbidity (in terms of NTU; HACH, 2100P, USA), a total organic carbon (Systematic, Model 1030W, USA), and total solids (TS), were determined using ROC EPA standard methods [24].

2.2. Methods and analysis

Before each experiment, the electrodes were polished with sandpaper to remove scale, dipped in 3 M H_2SO_4 to a depth of 6 cm for 10 min, and then cleaned with deionized water [25]. A circular container with 0.5 L of oxide-CMP wastewater was used as the reactor. The magnetic stirrer was turned on and set at 300 rpm. The stirrer speed was fast enough to provide good mixing in the electrolytic cell and yet slow enough to not break up the flocs formed during the process. A fixed amount of NaCl (0.002N) was added to the oxide-CMP wastewater to increase the conductivity and facilitate the EC process. The direct current power source was operated at a constant current density of 2.4, 3.2, 4.8, or 6.8 mA cm^{-2}. A steady temperature was maintained and ranged in this study from 288 to 318 K. The EC test run lasted 80 min for all of the experiments. Particulates of colloidal ferric hydroxide were produced, turning the aqueous solution a yellow-brown color after EC. Samples were periodically taken from the reactor and deposited for 6 h in a 20 ml Pyrex glass column. The COD concentration in the aqueous solutions was measured using a HACH Model DR2800 spectrophotometer (HACH Company, USA), and the analysis was conducted using the procedure described in Standard Methods [26]. The COD removal efficiency after the electrocoagulation treatment was calculated using:

$$\text{COD removal efficiency}\,(\%) = \frac{\text{COD}_0 V_0 - \text{COD}_t V_t}{\text{COD}_0 V_0} \times 100 \quad (1)$$

where COD_0 is the initial concentration in mg L^{-1}, COD_t is the concentration value at time t in mg L^{-1}, V_0 is the initial volume of the treated wastewater in liters, and V_t is the volume of the treated wastewater at time t in liters.

2.3. Properties of oxide-CMP wastewater

The oxide-CMP wastewater had a diluted milky appearance with a high total solids content of 4000–5000 mg L^{-1}, a suspended solids (SS) concentration of 10–20 mg L^{-1}, turbidity in the range of 200–300 NTU, TOC of 2–4 mg L^{-1}, a COD of 400–600 mg L^{-1}, a conductivity of 100–200 μs cm^{-1}, a pH of between 8 and 9, zeta potential of between −28 mV and −35 mV, and a mean particle size between 85 nm and 95 nm. All samples were measured in duplicate to ensure data reproducibility, and an additional measurement was carried out if necessary.

3. Results and discussion

3.1. Adsorption kinetics

The adsorption kinetics that describes the solute uptake rate and governs the residence time of the adsorption reaction is one of the important characteristics that define the adsorption efficiency. In this study, the COD removal kinetics from oxide-CMP wastewater was determined to observe the adsorption behavior of metal hydroxides generated during EC process.

3.1.1. Adsorption kinetics at different current densities

The current density is an important factor that strongly affects the performance of EC [27]. Current density was calculated as the applied current divided by the projected surface area of the studied electrode. Fig. 2 shows the effect of the current density on the COD removal efficiency for various electrolysis durations. As the duration of electrolysis increased, comparable increases in the COD removal efficiency were observed for all current densities. As shown in Fig. 2, after 50 min of electrolysis time, 68.3%, 81.1%, 90.7%, and 91.8% of the original COD was removed for current densities of 2.4, 3.2, 4.8, and 6.4 mA cm^{-2}, respectively. As the current density increased, the COD removal rate also increased. Furthermore, the amount of COD removal depends on the quantity of metal hydroxides generated, which is related to the time and current density. The results indicate that the current density determines the coagulant dosage rate. The required treatment times to reach over 90%

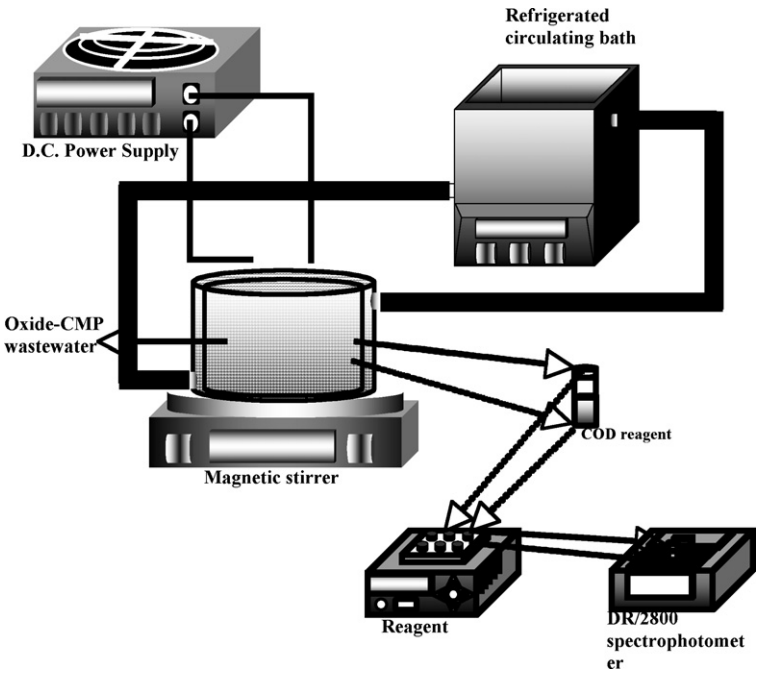

Fig. 1. Schematic diagram of the experimental setup.

of the COD removal were 80, 66, 49, and 45 min for 2.4, 3.2, 4.8, and 6.4 mA cm^{-2}, respectively. As the current density increased, the required time for the EC process decreased. When there is a sufficient level of current passing through the solution, the metal ions generated by the dissolution of the sacrificial electrode, hydrolyze and form a series of metallic hydroxides. These metallic hydroxides neutralize the electrostatic charges on the dispersed particles, thereby reducing the electrostatic interparticle repulsion so that the van der Waals attraction dominated and facilitated agglomeration [28]. However, no significant improvement in the COD removal efficiency for any duration of electrolysis was observed when the current density was increased from 4.8 to 6.4 mA cm^{-2}. To investigate the optimum current, the performance of the electric energy consumption at a certain current density during EC was evaluated. The electrical energy consumption required achieving the desired degree of treatment, rather than the highest removal efficiency, determines the feasibility of the proposed treatment approach. Once the required currents and corresponding voltages were obtained from EC experiments, the amount of energy used was estimated. The oxide-CMP wastewater was treated by iron EC for current densities in the range from 2.4 to 6.4 mA cm^{-2} after 50 min of electrolysis to determine the optimal COD removal efficiency and the associated electrical energy consumption. The effect of the current density and charge density on the COD removal efficiency and electrical energy consumption are shown in Fig. 3(a) and (b). Fig. 3(a) shows that increasing the current density from 2.4 to 6.4 mA cm^{-2} increased the COD removal efficiency from 68.3% to 91.8%. When the current density was increased from 3.2 to 4.8 mA cm^{-2}, the COD removal efficiency of oxide-CMP wastewater increased from 80.1% to 90.7%, whereas the corresponding electric energy consumption increased only slightly. However, when the current density was increased from 4.8 to 6.4 mA cm^{-2}, the COD removal efficiency increased slightly from 90.7% to 91.8%, whereas the corresponding electric energy consumption increased by almost a factor of two. So does the same tendency shown in Fig. 3(b). Accordingly, a current density of 4.8 mA cm^{-2} was chosen as the optimum current density for the following experiments.

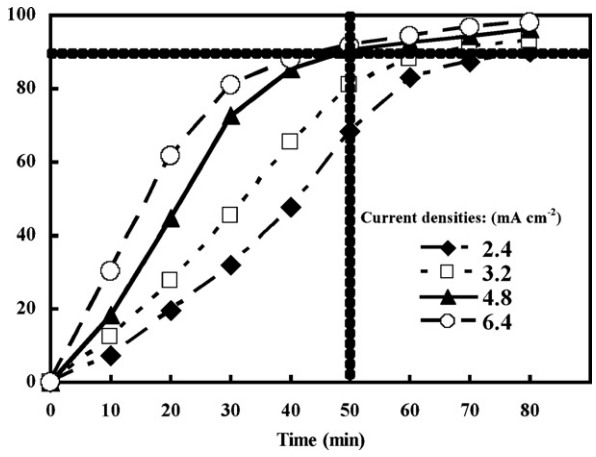

Fig. 2. Effect of current density on the COD removal efficiency (NaCl = 0.002N, T = 298 K, d = 2 cm and agitation speed = 300 rpm).

3.1.2. Adsorption kinetics at different temperatures

The effect of temperature on EC has not thoroughly been investigated even though EC technology has been used for more than 100 years. The effect of temperature on the COD removal efficiency of oxide-CMP wastewater was studied at 288, 298, 308, and 318 K, as shown in Fig. 4. As the electrolysis time increased, comparable increases in the COD removal efficiency were observed for the different temperatures. After 50 min of electrolysis, we observed that the COD removal efficiency reached 87.3%, 90.7%, 94.7%, and 96.3% for a temperature of 288, 298, 308, and 318 K, respectively. The treatment time required to reach 80% COD removal was approximately 27, 30, 35, and 39 min for a temperature of 318, 308, 298, and 288 K, respectively. The increase in the COD removal rate with increased temperatures can be attributed to the increased destruction of the passivation film on the anode surface and increased rates for all of the reactions involved in the process, according to the Arrehenius equation [27]. Additionally, the increased temperature promotes the generation of metal hydroxides in the EC process. The increase in metal hydroxides leads to an increase in their mobility and more frequent collisions, resulting in an increased reaction

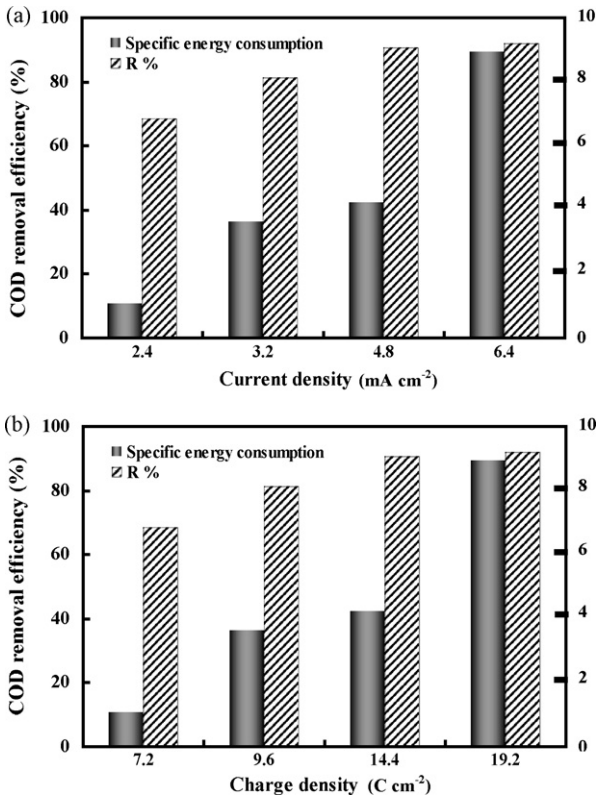

Fig. 3. Effect of (a) current density and (b) charge density on the COD removal efficiency and specific energy consumption (NaCl = 0.002N, t = 50 min, T = 298 K, d = 2 cm and agitation speed = 300 rpm).

rate between the metal hydroxides (i.e., iron hydroxides) and pollutants by adsorption [29]. As a result, the COD removal efficiency of oxide-CMP wastewater increases with increasing temperature.

3.2. Adsorption kinetic modeling

The pollutant is generally adsorbed at the surface of the metal hydroxides generated during the EC process. Thus the removal of pollutant is similar to conventional adsorption, except coagulants are generated. Coagulated particles attract and absorb different ions and colloidal particles from the wastewater. If iron electrodes are used, the generated Fe ions immediately undergo further spontaneous reactions to produce corresponding hydroxides and/or

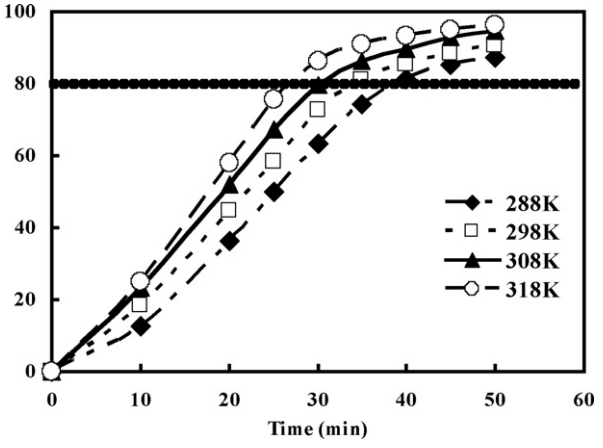

Fig. 4. Effect of temperature on the COD removal efficiency (current density = 4.8 mA cm^{-2}, NaCl = 0.002N, d = 2 cm and agitation speed = 300 rpm).

polyhydroxides. Ferric ions are commonly generated by oxidizing ferrous ions produced at the anode during the dissolution of iron, while OH^- ions are generated at the cathode. Mixing the solution produces hydroxide species, which remove pollutants by adsorption and co-precipitation. $Fe(OH)_3$ is the dominant species in the range from pH 6 to 10, according to predominance-zone diagrams for Fe(III) chemical species in aqueous solution [30]. In the present study, the pH values of oxide-CMP wastewater were varied from 7.5 (initial) to 9.5 (final) during the EC process, which indicates that $Fe(OH)_3$ is the dominant metal hydroxide functioning as an adsorbent. The corresponding voltage was varied from 7.7 V (initial) to 11.5 V (final) during the EC process. The electrode consumption can be estimated according to Faraday's law, and the amount of generated metal hydroxides can be stoichiometrically determined. Since the amount of coagulant can be estimated for a given time, the pollutant removal can be modeled using an adsorption phenomenon. The metal hydroxides formed during EC possess adsorption abilities. The amount of COD adsorbed by the $Fe(OH)_3$ in oxide-CMP wastewater was calculated from the difference between the COD quantity added to the $Fe(OH)_3$ and the COD content of the precipitation using the following equation:

$$q_e = \frac{V(C_0 - C_e)}{M} \tag{2}$$

where q_e is the COD uptake (mg g^{-1}), C_0 and C_e are, respectively, the initial and final or equilibrium COD concentrations in the solution (mg L^{-1}), V is the volume of the solution (L) and M is the mass of $Fe(OH)_3$ (s). In order to investigate the mechanisms of the COD adsorption process, two different kinetic models, the pseudo-first-order model and pseudo-second-order model, were applied to describe the kinetics of the COD adsorption onto iron hydroxides. The best-fit model was selected according to the linear regression correlation coefficient values, R^2.

3.2.1. Pseudo-first-order model

The first-order rate equation of the Lagergren model is one of the most widely used expression describing the adsorption of solute from a solution [31]. The pseudo-first-order equation is given by

$$\frac{dq_t}{dt} = k_1(q_e - q_t) \tag{3}$$

where q_e (mg g^{-1}) and q_t (mg g^{-1}) are the amounts of COD adsorbed on the adsorbent at equilibrium and at any time t, respectively, and k_1 (min^{-1}) is the rate constant of the pseudo-first-order model. After integration of Eq. (3) and applying the boundary conditions $q_t = 0$ at $t = 0$ and $q_t = q_t$ at $t = t$, we obtain:

$$\ln(q_e - q_t) = \ln\ q_e - k_1 t \tag{4}$$

The pseudo-first-order model considers the rate of occupation of the adsorption sites proportional to the number of unoccupied sites. The values of k_1 and q_e can be obtained from the slope and intercept of the linear plot of $\ln(q_e - q_t)$ versus t, respectively. The adsorption rate constants determined from the pseudo-first-order model for various current densities and temperatures are listed in Tables 1 and 2, respectively.

3.2.2. Pseudo-second-order model

The pseudo-second-order kinetic model is based on the adsorption equilibrium written as [32]:

$$\frac{dq}{dt} = k_2(q_e - q_t)^2 \tag{5}$$

where k_2 (g mg^{-1} min^{-1}) is the rate constant of the pseudo-second-order equation, q_e is the maximum adsorption capacity, and q_t is the amount of adsorption at time t. After integration and apply-

Table 1
Comparison of the pseudo-first-order and pseudo-second-order for different current densities.

Current density ($mA\,cm^{-2}$)	$q_{e,exp}$ ($mg\,g^{-1}$)	First-order model			Second-order model		
		$k_1 \times 10^2$ (min^{-1})	$q_{e,fit}$ ($mg\,g^{-1}$)	R^2	$k_2 \times 10^3$ ($L\,mg^{-1}\,min^{-1}$)	$q_{e,fit}$ ($mg\,g^{-1}$)	R^2
2.4	1512.3	4.83	1394.6	0.86	0.82	1533.2	0.97
3.2	1243.2	5.32	1030.9	0.91	1.31	1267.2	0.97
4.8	989.2	5.72	936.2	0.93	1.85	1004.6	0.98
6.4	862.7	5.93	829.4	0.94	2.84	871.8	0.99

Table 2
Comparison of the pseudo-first-order and pseudo-second-order for different temperatures.

Temperature (K)	$q_{e,exp}$ ($mg\,g^{-1}$)	First-order model			Second-order model		
		$k_1 \times 10^2$ (min^{-1})	$q_{e,fit}$ ($mg\,g^{-1}$)	R^2	$k_2 \times 10^3$ ($L\,mg^{-1}\,min^{-1}$)	$q_{e,fit}$ ($mg\,g^{-1}$)	R^2
288	939.7	4.99	889.5	0.85	1.74	957.9	0.95
298	989.2	5.72	936.2	0.93	1.85	1004.6	0.98
308	1011.1	8.54	951.6	0.92	1.88	1027.5	0.98
318	1040.6	9.93	1014.3	0.94	1.94	1048.9	0.99

ing the boundary conditions, $q_t = 0$ at $t = 0$ and $q_t = q_t$ at $t = t$, Eq. (5) becomes:

$$\frac{t}{q_t} = \frac{1}{k_2 q_e^2} + \frac{t}{q_e} \tag{6}$$

As discussed above, the validity of the Lagergren and the pseudo-second-order kinetic models can be identified from each linear plot. If second-order kinetics model is applicable, plotting t/q_t as a function of t will result in a straight line, and q_e and k_2 can be obtained from its slope and intercept, respectively. As shown in Figs. 5 and 6, the plots of t/q_t versus t yield relatively straight lines for the different current densities and temperatures. Furthermore, the correlation coefficients, R^2, for the pseudo-second-order kinetic model obtained in all cases were above 0.97 and the calculated q_e values agreed with the experimental q_e values. The adsorption rate constants determined from the pseudo-second-order model for the different current densities and temperatures are also listed in Tables 1 and 2, respectively. We observed that the correlation coefficients for the first-order kinetic model were relatively lower than those obtained for the second-order kinetic model for the different current densities and temperatures. These results indicate that the second-order kinetic model can be applied suitably to predict the COD adsorption process onto iron hydroxides.

3.3. Adsorption isotherms

These gelatinous charged hydroxides generated during EC process can effectively remove pollutants by adsorption and produce charge neutralization by complexation, electrostatic attraction, and precipitation [33]. To identify the mechanism of the adsorption process, it is important to establish the most appropriate correlation for the equilibrium curves. In this study, three adsorption isotherms, Langmuir, Freundlich, and Dubinin–Raduskevich (D–R), were applied to establish the relationship between the amounts of COD adsorbed onto the iron hydroxides and its equilibrium concentration in oxide-CMP wastewater.

3.3.1. Langmuir isotherm

The Langmuir model was originally developed to represent chemisorption at a set of well-defined localized adsorption sites with the same adsorption energy, independent of the surface coverage, and with no interaction between adsorbed molecules. This model assumes a monolayer deposition on a surface with a finite number of identical sites. The mathematical expression for the Langmuir isotherm is [34]:

$$q_e = \frac{a_L K_L C_e}{1 + K_L C_e} \tag{7}$$

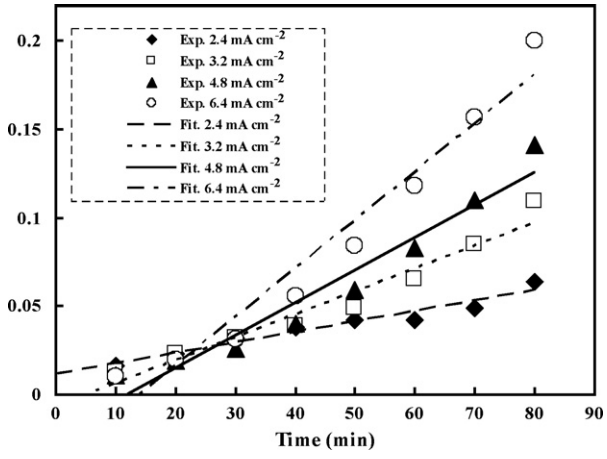

Fig. 5. Comparison between the experimental and calculated q_e values for different current densities in pseudo-second-order kinetic model at temperature 298 K.

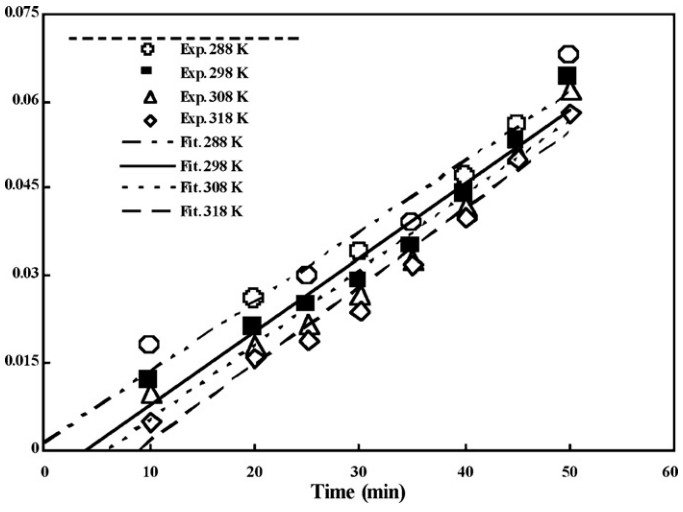

Fig. 6. Comparison between the experimental and calculated q_e values for different temperatures in pseudo-second-order kinetic model at current density 4.8 $mA\,cm^{-2}$.

Table 3
Langmuir and Freundlich and Dubinin–Radushkevich (D–R) isotherm constants for the COD adsorption onto iron hydroxides.

Langmuir		Freundich		Dubinin–Radushkevich (D–R)	
K_L (L mg^{-1})	0.0214	K_F ((mg g^{-1}) (L mg^{-1})$^{1/n}$)	4.194	q_m (mg g^{-1})	876
a_L (mg g^{-1})	1667	n	0.664	k (mol^2 (kJ^2)$^{-1}$)	0.03
				E (kJ mol^{-1})	4.08
R^2	0.97	R^2	0.99	R^2	0.87

where a_L (mg g^{-1}) is a constant related to the area occupied by a monolayer of adsorbate, reflecting the maximum adsorption capacity; C_e (mg L^{-1}) is the equilibrium liquid-phase concentration; K_L (L mg^{-1}) is a direct measure of the intensity of adsorption; and q_e (mg g^{-1}) is the amount adsorbed at equilibrium. This equation can be linearized as

$$\frac{1}{q_e} = \left(\frac{1}{K_L a_L}\right)\left(\frac{1}{C_e}\right) + \frac{1}{a_L} \quad (8)$$

From the plot of $1/q_e$ versus $1/C_e$, K_L and a_L can be determined from the slope and intercept of the resulting straight line.

3.3.2. Freundlich isotherm

The Freundlich adsorption isotherm is typically an empirical model, which includes the surface heterogeneity and exponential distribution of the active sites and their energies. The isotherm is adopted to describe reversible adsorption and is not restricted to a monolayer formation. The mathematical expression for the Freundlich mode is [35]:

$$q_e = K_f C_e^{1/n} \quad (9)$$

where K_f ((mg g^{-1}) (L mg^{-1})$^{1/n}$) and n (dimensionless) are constants that account for all factors affecting the adsorption process, such as the adsorption capacity and intensity. This equation can be linearized, resulting in:

$$\ln\ q_e = \ln K_f + \frac{1}{n}\ln C_e \quad (10)$$

The Freundlich constants K_f and $1/n$ are determined from the intercept and slope, respectively, of the linear plot of $\ln q_e$ versus $\ln C_e$.

3.3.3. Dubinin–Raduskevich (D–R) isotherm

The D–R isotherm is an empirical adsorption model on a single type of uniform pores [36]. It is applied to describe the adsorption mechanism with a Gaussian energy distribution onto a heterogeneous surface [37,38]. The mathematical expression for the D–R isotherm is

$$q_e = q_m e^{-k\varepsilon^2} \quad (11)$$

The linear form of the (D–R) isotherm equation is:

$$\ln\ q_e = \ln q_m - k\varepsilon^2 \quad (12)$$

where ε (Polanyi potential) is $[RT\ln(1 + 1/C_e)]$, R, T and C_e represent the gas constant (J mol^{-1} K^{-1}), absolute temperature (K) and adsorbate equilibrium concentration (mg L^{-1}), q_e is the amount of solute adsorbed per unit weight of adsorbent (mg g^{-1}), k is a constant related to the adsorption energy (mol^2 kJ^{-2}), and q_m is the adsorption capacity (mg g^{-1}). By plotting $\ln q_e$ versus ε^2, it is possible to estimate the value of q_m from the intercept and the value of k from the slope. The constant k gives an idea about the mean free energy E (kJ mole^{-1}) of adsorption, which can be calculated using the relationship:

$$E = \frac{1}{\sqrt{2k}} \quad (13)$$

The magnitude of E provides useful information for estimating the adsorption mechanism. In the case of $E < 8$ kJ mole^{-1}, physical forces may affect the adsorption. For E in the range of 8–16 kJ mole^{-1}, ion exchange is the working mechanism. While for $E > 16$ kJ mole^{-1} adsorption may be dominated by particle diffusion [39]. In this study, the E value is calculated as 4.08 kJ mole^{-1}, which indicates the physical nature of COD adsorption onto iron hydroxides.

The applicability of the isotherm equations was compared using the correlation coefficient (R^2). The Langmuir, Freundlich and D–R isotherm constants for the adsorption of COD onto iron hydroxides are presented in Table 3. The Freundlich isotherm model provided a better fit to the experimental data ($R^2 = 0.99$) based on comparison of the R^2 values for the COD adsorption onto iron hydroxides. The variable K_f in the Freundlich equation is related to the adsorption capacity of the adsorbent and n gives the deviation extent from linearity of the adsorption. When the value of n is equal to unity, the adsorption sites have equal energy and no interaction occurs between the adsorbed species. If $n < 1$, the adsorption process is largely physical. If $n > 1$, the adsorption process is chemical [40]. Since the value of n at equilibrium was 0.664 at 298 K in this study, physical adsorption was dominant for the COD adsorption onto iron hydroxides.

3.4. Adsorption thermodynamics

Thermodynamic parameters, including Gibbs free energy change (ΔG°), enthalpy change (ΔH°), and entropy change (ΔS°), were used to determine whether or not the adsorption process was spontaneous. The values of ΔG° were calculated using the following equation:

$$\Delta G^\circ = -RT\ln K_d \quad (14)$$

where R is the gas constant (8.314 J mol^{-1} K^{-1}), T is the temperature (K), and K_d is the distribution coefficient. The K_d value was calculated using the following equation [41]:

$$K_d = \frac{q_e}{C_e} \quad (15)$$

where q_e and C_e are the equilibrium concentrations of COD for the adsorbent (mg L^{-1}) and the solution (mg L^{-1}), respectively. The relationship between ΔG°, ΔH° and ΔS° can be expressed by the following equation:

$$\Delta G^\circ = \Delta H^\circ - T\Delta S^\circ \quad (16)$$

Combining Eqs. (14) and (16) leads to:

$$\ln\ K_d = \frac{\Delta S^\circ}{R} - \frac{\Delta H^\circ}{RT} \quad (17)$$

The temperature effect on the adsorption efficiency of the COD for CMP wastewater was evaluated at different temperatures ranging from 288 to 318 K. For the different temperatures, the corresponding C_e values at different fixed values of q_e were calculated. The thermodynamic parameters of ΔH° and ΔS° were calculated from the slope and intercept of the plot of $\ln K_d$ versus $1/T$, respectively, as shown in Fig. 7. The Gibbs free energies at different temperatures were calculated from Eq. (14). The values of ΔG°, ΔH°, and ΔS° for the COD adsorption onto iron hydroxides at different temperatures are given in Table 4. At all temperatures, ΔG° is

Table 4
Thermodynamic parameters for the COD adsorption onto iron hydroxides at different temperatures.

Temperature (K)	K_d	ΔG° (kJ mol^{-1} K^{-1})	ΔS° (kJ mol^{-1} K^{-1})	ΔH° (kJ mol^{-1})
288	3.036	−7.112	0.145	34.63
298	3.378	−8.369		
308	4.004	−10.253		
318	4.342	−11.480		

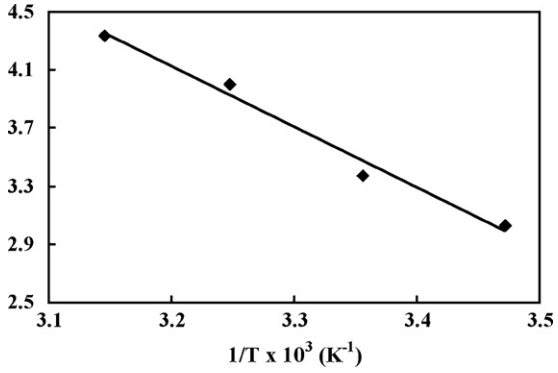

Fig. 7. Plot of $\ln K_d$ versus $1/T$ for the estimation of thermodynamic parameters for the COD adsorption onto iron hydroxides.

negative, indicating the feasibility of the process and spontaneous nature of the adsorption of COD on iron hydroxides. The increase in the absolute magnitude of ΔG° with increasing temperatures indicates that these processes were favored at high temperatures. The positive value of ΔH° indicates that the adsorption process is endothermic. In addition, the positive value of ΔS° suggests increased randomness at the solid–solution interface during the COD adsorption of oxide-CMP wastewater on iron hydroxides. While the adsorption process was endothermic under these conditions, the process was spontaneous owing to the positive entropy change.

4. Conclusion

This study indicated that EC is a promising treatment for the COD removal from oxide-CMP wastewater from a semiconductor manufacturing plant and showed the feasibility of removing COD by adsorption with iron hydroxides. The following conclusions were obtained:

(1) The COD removal efficiency from oxide-CMP wastewater was significantly influenced by the current density and temperature for the present EC study.
(2) The pseudo-first-order model and pseudo-second-order model were applied to identify the kinetics of COD adsorption onto iron hydroxides. The kinetic results showed that the COD adsorption of oxide-CMP wastewater on iron hydroxides was best described using the pseudo-second-order kinetic model at the various current densities and temperatures.
(3) The gelatinous and charged metal hydroxides generated by EC can efficiently remove COD by adsorption, and the EC process was modeled using adsorption isotherm models. The COD adsorption of oxide-CMP wastewater fit the Freundlich adsorption isotherm best and the results were in good agreement with the experimental data.
(4) Thermodynamic parameters (ΔG°, ΔH° and ΔS°) were also determined. Their values indicated that the adsorption process was favorable, spontaneous, and endothermic in nature. As the temperature increased from 288 to 318 K, ΔG° became less negative, indicating more of a driving force and hence resulting in a greater adsorption capacity at higher temperatures. The positive value of ΔH° confirmed that the process was endothermic, meaning that the reaction consumed energy. The positive value of ΔS° suggested that the increased randomness at the interface during the COD adsorption onto iron hydroxides.
(5) Under the prevailing conditions, the COD removal was better than 90% with a final COD concentration below the Taiwan discharge standard (100 mg L^{-1}). The wastewater quality exceeded the direct discharge standard, and the effluent could be considered for reuse.

Acknowledgement

The authors would like to thank the National Science Council, Taiwan, ROC for financially supporting this study under contract number NSC98-2622-E-241-018-CC3.

References

[1] Y.G. Wang, Y.W. Zhao, W. An, J. Wang, Modeling the effects of cohesive energy for single particle on the material removal in chemical mechanical polishing at atomic scale, Appl. Surf. Sci. 253 (2007) 9137–9141.
[2] G.C.C. Yang, CMP wastewater management using the concepts of design for environment, Environ. Prog. 21 (2002) 57–62.
[3] J.H. Golden, J.E. Carrubba, Chemistry of CMP wastewater, Semicond. Fabtech. 13 (2001) 123–126.
[4] J.H. Golden, R. Small, L. Pagan, C. Shang, S. Ragavan, Evaluating and treating CMP wastewater, Semicond. Int. 23 (2000) 85–98.
[5] L.J.J. Janssen, L. Koene, The role of electrochemistry and electrochemical technology in environmental protection, Chem. Eng. J. 85 (2002) 137–146.
[6] C.L. Lai, S.H. Lin, Electrocoagulation of chemical mechanical polishing (CMP) wastewater from semiconductor fabrication, Chem. Eng. J. 95 (2003) 205–211.
[7] M. Kobya, H. Hiz, E. Senturk, C. Aydiner, E. Demirbas, Treatment of potato chips manufacturing wastewater by electrocoagulation, Desalination 190 (2006) 201–211.
[8] P.K. Holt, G.W. Barton, M. Wark, C.A. Mitchell, A quantitative comparison between chemical dosing and electrocoagulation, Colloid Surf. A211 (2002) 233–248.
[9] M.T. Pouet, A. Grasmick, Urban wastewater treatment by electrocoagulation and flotation, Water Sci. Technol. 31 (1995) 275–283.
[10] I. Heidmann, W. Calmano, Removal of Zn(II), Cu(II), Ni(II), Ag(I) and Cr(VI) present in aqueous solutions by aluminum electrocoagulation, J. Hazard. Mater. 152 (2008) 934–941.
[11] N. Daneshvar, A. Oladegaragoze, N. Djafarzadeh, Decolorization of basic dye solutions by electrocoagulation: an investigation of the effect of operational parameters, J. Hazard. Mater. B84 (2006) 116–122.
[12] X. Chen, G. Chen, L.Y. Po, Separation of pollutants from restaurant wastewater by electrocoagulation, Sep. Purif. Technol. 19 (2000) 65–76.
[13] C.T. Wang, W.L. Chou, L.S. Chen, S.Y. Chang, Silica particles settling characteristics and removal performances of oxide chemical mechanical polishing wastewater treated by electrocoagulation technology, J. Hazard. Mater. 161 (2009) 344–350.
[14] W.L. Chou, C.T. Wang, S.Y. Chang, Study of COD and turbidity removal from real oxide-CMP wastewater by iron electrocoagulation and the evaluation of specific energy consumption, J. Hazard. Mater. 168 (2009) 1200–1207.
[15] C.T. Wang, W.L. Chou, Performance of COD removal from oxide chemical mechanical polishing wastewater using iron electrocoagulation, J. Environ. Sci. Health, Part A 44 (12) (2009) 1289–1297.
[16] Ş. İrdemez, N. Demircioğlu, Y.Ş. Yildiz, Z. Bingül, The effects of current density and phosphate concentration on phosphate removal from wastewater by electrocoagulation using aluminum and iron plate electrodes, Sep. Purif. Technol. 52 (2006) 218–223.
[17] N. Mameri, H. Lounici, D. Belhocine, H. Grib, D.L. Piron, Y. Yahiat, Defluoridation of Sahara water by small plant electrocoagulation using bipolar aluminum electrodes, Sep. Purif. Technol. 24 (2001) 113–119.
[18] J.R. Parga, D.L. Cocke, J.L. Valenzuela, J.A. Gomes, M. Kesmez, G. Irwin, H. Moreno, M. Weir, Arsenic removal via electrocoagulation from heavy metal contaminated groundwater in La Comarca Lagunera Mexico, J. Hazard. Mater. B124 (2005) 247–254.

[19] W.L. Chou, C.T. Wang, K.Y. Huang, Effect of operating parameters on indium (III) ion removal by iron electrocoagulation and evaluation of specific energy consumption, J. Hazard. Mater. 167 (2009) 467–474.
[20] W.L. Chou, Y.-H. Huang, Electrochemical removal of indium ions from aqueous solution using iron electrodes, J. Hazard. Mater. 172 (2009) 46–53.
[21] W.L. Chou, C.T. Wang, K.Y. Huang, Investigation of process parameters for the removal of polyvinyl alcohol from aqueous solution by iron electrocoagulation, Desalination 251 (2010) 12–19.
[22] C.T. Wang, W.L. Chou, K.Y. Huang, Treatment of polyvinyl alcohol from aqueous solution via electrocoagulation, Sep. Sci. Technol. 45 (2010) 212–220.
[23] W.L. Chou, Removal and adsorption characteristics of polyvinyl alcohol from aqueous solutions using iron electrocoagulation, J. Hazard. Mater. 177 (2010) 842–850.
[24] ROC Environmental Protection Administration (EPA), Standard Environmental Methods for Water Quality, 2007 (in Chinese) http://www.niea.gov.tw/niea/WATER/.
[25] P.R. Kumar, S. Chaudhari, K.C. Khilar, S.P. Mahajan, Removal of arsenic from water by electrocoagulation, Chemosphere 55 (2004) 1245–1252.
[26] American Public Health Association (APHA), Standard Methods for the Examination of Water and Wastewater, 17th ed., APHA, Washington, DC, 1992.
[27] D. Pletcher, F.C. Walsh, Industrial Electrochemistry, 2nd ed., Blackie Academic & Professional, London, UK, 1990.
[28] M.Y.A. Mollah, R. Schennach, J. Parga, D.L. Cocke, Electrocoagulation (EC)-science and applications, J. Hazard. Mater. B84 (2001) 29–41.
[29] E.S.Z. El-Ashtoukhy, N.K. Amin, O. Abdelwahab, Treatment of paper mill effluents in batch-stirred electrochemical tank reactor, Chem. Eng. J. 146 (2009) 205–210.
[30] I.A. Sengil, M. Özacar, B. Ömürlü, Decolorization of C.I. reactive red 124 using the electrocoagulation method, Chem. Biochem. Eng. Quart. 18 (2004) 273–277.
[31] S. Lagergren, About the theory of so-called adsorption of soluble substance, Kung Sven. Veten. Hand 24 (1898) 1–39.
[32] Y.S. Ho, G. McKay, Kinetic models for the sorption of dye from aqueous solution by wood, J. Environ. Sci. Health Part B: Process. Saf. Environ. Prot. 76 (1998) 183–191.
[33] M.Y.A. Mollah, R. Schennach, J.R. Parga, D.L. Cocke, Electrocoagulation (EC)-science and applications, J. Hazard. Mater. B84 (2001) 29–41.
[34] I. Langmuir, The constitution and fundamental properties of solids and liquids, J. Am. Chem. Soc. 38 (1916) 2221–2295.
[35] H.M.F. Freundlich, Over the adsorption in solution, J. Phys. Chem. 57 (1906) 385–471.
[36] M.M. Dubinin, L.V. Radushkevich, The equation of the characteristic curve of the activated charcoal, Proc. Acad. Sci. USSR Phys. Chem. Sect. 55 (1947) 331–337.
[37] A. Dabrowski, Adsorption—from theory to practice, Adv. Colloid Interface Sci. 93 (2001) 135–224.
[38] A. Çabuk, T. Akar, S. Tunali, Ö. Tabak, Biosorption characteristics of Bacillus sp. ATS-2 immobilized in silica gel for removal of Pb(II), J. Hazard. Mater. B136 (2006) 317–323.
[39] S. Ahmad, N. Khalid, M. Daud, Adsorption studies of lead on lateritic minerals from aqueous media, Sep. Sci. Technol. 37 (2) (2002) 343–362.
[40] J.Q. Jiang, C. Cooper, S. Quki, Comparison of modified montmorillonite adsorbents. Part I. Preparation, characterization and phenol adsorption, Chemosphere 47 (2002) 711–716.
[41] E.I. Unuabonah, K.O. Adebowale, B.I. Olu-Owolabi, Kinetic and thermodynamic studies of the adsorption of lead (II) ions onto phosphate modified kaolinite clay, J. Hazard. Mater. 144 (2007) 386–395.